

# **The influence of carbon surface chemical composition on Dubinin - Astakhov equation parameters calculated from SF<sub>6</sub> adsorption data – GCMC simulation**

Sylwester Furmaniak<sup>(1)</sup>, Artur P. Terzyk<sup>(1,\*)</sup>, Piotr A. Gauden<sup>(1)</sup>, Piotr  
Kowalczyk<sup>(2)</sup>, Peter J.F. Harris<sup>(3,\*)</sup>

*(1) N. Copernicus University, Department of Chemistry, Physicochemistry of Carbon  
Materials Research Group, Gagarin St. 7, 87-100 Toruń, Poland,*

*(2) Nanochemistry Research Institute, Curtin University, PO Box U1987, Perth WA 6845,  
Australia*

*(3) Centre for Advanced Microscopy, University of Reading, Whiteknights,  
Reading RG6 6AF, UK*

*(\*) corresponding author*

Artur P. Terzyk

N. Copernicus University  
Physicochemistry of Carbon Materials Research Group  
Department of Chemistry  
Gagarina St. 7  
87-100 Toruń  
Poland  
e-mail: aterzyk@chem.uni.torun.pl  
url: <http://www.chem.uni.torun.pl/~aterzyk/>

Peter J.F. Harris

Centre for Advanced Microscopy,  
University of Reading,  
Whiteknights,  
Reading RG6 6AF, UK

**Abstract:** Using GCMC simulation we show, for the first time, the influence of carbon porosity and surface oxidation on the parameters of the DA adsorption isotherm equation. We conclude that after carbon surface oxidation adsorption decreases for all studied carbons. Moreover, the parameters of the DA model depend on the number of surface oxygen groups. That is the reason why in the case of carbons containing surface polar groups SF<sub>6</sub> adsorption isotherm data cannot be applied for characterisation of porosity.

**Keywords:** adsorption, activated carbon, GCMC simulation

## 1. Introduction

In a recently published study Chiang and Wu [1] pointed out that the application of SF<sub>6</sub> in the electrical industry, semiconductor, aluminium smelting and magnesium industries, as well in medicine is due to its low toxicity, high thermal stability and high breakdown strength. SF<sub>6</sub> is also a common tracer gas for use in experiments or oceanography. According to the Intergovernmental Panel on Climate Change, SF<sub>6</sub> is the most potent greenhouse gas [1]. An SF<sub>6</sub> admixture to freons decreases the boiling temperature of halones, and this property is used in refrigeration engineering [2].

Due to the large amount produced annually and its long atmospheric lifetime (ca. 3200 years) the use of SF<sub>6</sub> has recently become a global environmental issue. SF<sub>6</sub> is a perfluorochemical (PFC) and there are several ways to reduce and eliminate PFC emissions from industrial processes. Different authors proposed abatement/destruction methods however, common techniques for recovery/recycling of SF<sub>6</sub> are cryogenic condensation, adsorption, and membrane separation. Regarding adsorption an SF<sub>6</sub> isotherm is often applied for characterization of carbons (see for example [2,3]).

In the current study we present the results of GCMC simulation of SF<sub>6</sub> adsorption on realistic Virtual Porous Carbon (VPC) model of activated carbon proposed by Harris *et al.* [4-6]. It was shown previously that using this model it is possible for simulated data to obtain the same correlations as observed in real experiments [7]. Moreover, using this model we explained the meaning of some empirical parameters occurring in models applied for theoretical description of methane adsorption on carbons [8]. Moreover, this model was also successfully used for explanation of behaviour of carbons in adsorption of phenol from aqueous solutions [9].

For the reasons mentioned above we decided to check how the porosity and the chemical composition of the carbon surface layer determine the parameters obtained from description of SF<sub>6</sub> adsorption data by the most popular adsorption isotherm equation, namely the Dubinin - Astakhov one. Since it is impossible to check this experimentally we decided to use a realistic VPC model (where the geometric, i.e. absolute, porosity is exactly known), and a molecular simulation technique applying one of the most advanced models of the SF<sub>6</sub> molecule.

## 2. Calculations details

### 2.1. Simulation boxes

We used four series of VPCs generated based on the (above-mentioned) Harris model and described in detail previously [10,11]. The series were obtained by introduction of surface carbonyl groups (using, the so called “virtual oxidation” procedure developed by us [10]) into four generated VPCs [12], denoted as S00 (S0), S12, S20, S35. These structures differ in porosity (see [12]). This “absolute” (geometric) porosity was calculated using the method proposed by Bhattacharya and Gubbins [13] and described previously (see for example [10,11]). Structure S00 has the widest pores, and the average pore size decreases gradually down to structure S35. Structures are denoted as Sxx\_yyy, where Sxx denotes starting structure and yyy denotes the number of carbonyl groups. We used following virtual carbons: (a) S00 series: S00\_000, S00\_036, S00\_072, S00\_108, S00\_144, S00\_180; (b) S12 series: S12\_000, S12\_050, S12\_100, S12\_150, S12\_200, S12\_250; (c) S20 series: S20\_000, S20\_058, S20\_116, S20\_174, S20\_232, S20\_290; and (d) S35 series: S35\_000, S35\_072, S35\_144, S35\_216, S35\_288, S35\_360. All structures were placed in cuboidal simulation box having dimensions 4.6 × 4.6 × 4.6 nm. As was shown in our previous papers [10,11] virtual oxidation practically does not change porosity (see below).

### 2.2. Grand Canonical Monte Carlo (GCMC) simulations

For all above-described structures the simulations of SF<sub>6</sub> adsorption at 298 K (in the range of pressures ca. 1 Pa up to ca. 2.32 MPa ( $p_s = 2.3568$  MPa [14])) using the standard GCMC method were performed [15]. The probability of attempts of changing of a state of a system by creation, annihilation, and rotation and displacement (the latter one is connected

with the change in angular orientation) were equal to: 1/3, 1/3, 1/6 and 1/6. For each adsorption point  $2.5 \times 10^7$  iterations were performed during the equilibration, and next  $2.5 \times 10^7$  equilibrium ones, applied for the calculation of the averages (one iteration = an attempt to change the state of the system by creation, annihilation, rotation or displacement). Enthalpy of adsorption was calculated from the theory of fluctuations.

The SF<sub>6</sub> molecule was modeled by the seven-centre rigid model [16]. Each centre was the (12,6) Lennard-Jones one (LJ) as well as the point charge ( $q$ ). We used the values of parameters of Strauss force field optimized by Dellis and Samios [16]. Values of parameters for the carbonaceous skeleton and atoms forming carbonyl groups were taken from [17]. The energy of interactions were calculated analogically as in our previous papers [10,18]. For all LJ-type interactions the cut-off is assumed as equal to  $r_{cut,ij} = 5 \times \sigma_{ij}$ . Tab. 1 collects all values of applied interaction parameters (we used the Lorentz-Berthelot mixing rules).

### 2.3 Description of simulated isotherms by the DA model

For a description of simulated adsorption isotherms we applied the Dubinin - Astakhov (DA) adsorption isotherm equation in the form:

$$a = a_0 \exp \left[ - \left( \frac{A}{E} \right)^n \right] \quad (1)$$

where:

$$A = RT \ln \frac{p_s}{p} \quad (2)$$

and  $a$  and  $a_0$  are the values of adsorption and maximum adsorption, respectively,  $p$  and  $p_s$  are the equilibrium pressure and saturated vapour pressure at a given temperature ( $T$ ),  $E$  is the characteristic energy of adsorption (multiplied by the affinity coefficient), and  $R$  is the gas constant.

Data were described using genetic algorithms proposed by Storn and Price [19] and applied by us previously (see for example [11,12,20,21]). The goodness of the fit was estimated using the values of the determination coefficients ( $DC$ ) - for details see for example [11].

### 3. Results and discussion

Fig. 1 shows the geometric (absolute) pore size distributions of the studied structures. As mentioned above all structures are microporous, structure S00 has dispersed microporosity, and the average micropore diameter decreases passing from S00 down to S35. Figure 1 also shows one important feature of the studied structures, namely, that after “virtual oxidation” of structures the porosity remains almost unchanged. Therefore we can conclude that the changes in SF<sub>6</sub> adsorption value (for a given series) are caused only by the changes in chemical composition of carbon surface layer and not by porosity.

Fig. 2 shows adsorption isotherms. As one can see the number of molecules in the simulation box increases with increasing number of oxygen groups in VPC model. This effect is visible especially at low pressures. The isosteric enthalpy of adsorption increases at the same time, and this is due to electrostatic interactions between oxygen and SF<sub>6</sub> molecules. However, due to the rise in the VPC mass after oxidation, the differences in adsorption isotherms become strongly pronounced if absolute adsorption is considered. This is also the reason why we observe a decrease in adsorption (at larger pressures) with a rise in a number of surface oxygen groups in VPC model.

In Fig.3 we compare the number of molecules in a simulation box and adsorption isotherms for VPC models differing in porosity. One can observe that the number of SF<sub>6</sub> molecules in the simulation box increases at low pressures with the rise in micropore diameter of carbon and decreases at larger pressures due to the decrease in the volume of adsorption space. If absolute adsorption is considered we observe that the smaller the average micropore diameter the smaller is the adsorption, and exactly the reverse effect is seen if one compares the relative adsorption, or the enthalpy plotted as a function of relative adsorption.

The major conclusion of this part of the study is that the oxidation of activated carbon leads to a decrease in SF<sub>6</sub> adsorption.

Finally in Figs.4 and 5 we show the results of a description of simulated data using the DA adsorption isotherm equation (Eq.1 and Tab.2), plotted as a function of oxygen content (Fig.4) and the converse of average micropore diameter (Fig.5). Since there are negligibly small changes in porosity after carbon oxidation (see Fig.1) it is obvious that the correlations observed on Fig.4 are caused by the interactions of adsorbed molecules with oxygen. We see that both the characteristic energy of adsorption as well as the parameter  $n$  of the DA model are affected by the number of oxygen groups present on carbon surface. Therefore as in the

case of nitrogen [10] and/or carbon dioxide [10,11] adsorption, it can be concluded that SF<sub>6</sub> adsorption data on microporous carbon, described by DA model, cannot be applied for microporosity characterisation if carbon contains oxygen surface functionalities. On the other hand, Fig. 5 shows that in fact for carbons not containing oxygen  $E$  is related to the micropore diameter. Therefore the characteristic adsorption energy of the DA model can be applied for calculation of the average micropore diameter but only if the new relation between those two values is developed, since as can be seen from Fig.5 also the parameter  $n$  of this equation is correlated with the average micropore diameter. Therefore, the application of simple inverse relationship between characteristic energy and pore diameter is questionable.

## CONCLUSIONS

We show, for the first time, the influence of carbon porosity and surface oxidation on the parameters of the DA adsorption isotherm equation. It is demonstrated that after carbon surface oxidation adsorption decreases for all studied carbons. Moreover, the parameters of the DA model depend on the number of surface oxygen groups. That is the reason why in the case of carbons containing surface polar groups SF<sub>6</sub> adsorption isotherm data described by DA model cannot be applied for characterisation of porosity. On the other hand if carbon does not contain polar surface groups a new relationship between  $E_0$  and pore diameter should be proposed, since the parameter  $n$  also depends on the pore diameter.

## Acknowledgements

The authors acknowledge the use of the computer cluster at Poznań Supercomputing and Networking Center and the Information and Communication Technology Center of the Nicolaus Copernicus University (Toruń, Poland). S.F. gratefully acknowledges the financial support from the Foundation for Polish Science.

## References

- [1] Chiang Y-C and Wu P-Y 2010 *J. Hazard. Mater.* **178** 729
- [2] Pribylov A A, Kalinnikova I A and Regent N I 2003 *Russ. Chem. Bull.* **52** 882
- [3] Cai Q, Buts A, Biggs M J and Seaton N A 2007 *Langmuir* **23** 8430
- [4] Harris P J F and Tsang S C 1997 *Phil. Mag. A* **76** 667
- [5] Harris P J F 1997 *Int. Mater. Rev.* **42** 206
- [6] Harris P J F 2005 *Crit. Rev. Solid State Mater. Sci.* **30** 235
- [7] Terzyk A P, Furmaniak S, Gauden P A, Harris P J F and Włoch J 2008 *J. Phys.: Condens. Matter* **20** 385212
- [8] Terzyk A P, Furmaniak S, Wesołowski R P, Gauden P A and Harris P J F 2010 *Advances in Adsorption Technology* ed B B Saha and K C Ng (New York: Nova Science Publishers) ch 14
- [9] Terzyk A P, Gauden P A, Furmaniak S, Wesołowski R P and Harris P J F 2010 *Phys. Chem. Chem. Phys.* **12** 812
- [10] Furmaniak S, Terzyk A P, Gauden P A, Harris P J F and Kowalczyk P 2009 *J. Phys.: Condens. Matter* **21** 315005
- [11] Furmaniak S, Terzyk A P, Gauden P A, Harris P J F and Kowalczyk P 2010 *J. Phys.: Condens. Matter* **22** 085003
- [12] Terzyk A P, Furmaniak S, Gauden P A, Harris P J F, Włoch J and Kowalczyk P 2007 *J. Phys.: Condens. Matter* **19** 406208
- [13] Bhattacharya S and Gubbins K E 2006 *Langmuir* **22** 7726
- [14] NIST Standard Reference Database Number 69 <http://webbook.nist.gov/chemistry/>
- [15] Frenkel D and Smit B 1996 *Understanding Molecular Simulation* (San Diego, CA: Academic)
- [16] Dellis D and Samios J 2010 *Fluid Phase Equilib.* **291** 81
- [17] Jorge M, Schumacher C and Seaton N A 2002 *Langmuir* **18** 9296.
- [18] Furmaniak S, Terzyk A P, Gauden P A and Kowalczyk P Simulation of SF<sub>6</sub> adsorption on the bundles of single walled carbon nanotubes (submitted)
- [19] Storn R and Price K 1997 *J. Global Optim.* **11** 341
- [20] Furmaniak S, Gauden P A, Terzyk A P and Rychlicki G 2008 *Adv. Colloid Interface Sci.* **137** 82
- [21] Furmaniak S, Terzyk A P, Gołembiewski R, Gauden P A and Czepirski L 2009 *Food Res. Int.* **42** 1203





**Table 1**

The values of LJ parameters and point charges located on the centres of studied systems.

molecule/structure	geometric parameters	centre	$\sigma$ [nm]	$\epsilon/k_B$ [K]	$q/e$	reference
<b>SF<sub>6</sub></b>	$l_{SF} = 0.1564$ nm	S	0.3228	165.14	+ 0.66	[16]
		F	0.2947	27.02	- 0.11	
<b>adsorbent</b>	$l_{CO} = 0.1233$ nm	C <sup>*)</sup>	0.3400	28.00	-	[17]
		C <sup>**)</sup>	0.3400	28.00	+ 0.50	
		O	0.2960	105.8	- 0.50	

\*) - non-carbonyl group atom of C

\*\*\*) - carbonyl group C atom

**Table 2**

The values of the best fit parameters obtained from the description of simulated isotherms using DA equation (Eqs. (1) and (2)).

<b>System</b>	<b><math>a_0</math> [molecules/box]</b>	<b><math>E</math> [kJ/mol]</b>	<b><math>n</math></b>	<b><math>DC</math></b>
<i>S00_000</i>	452.0	7.215	1.370	0.9986
<i>S00_036</i>	452.6	7.479	1.410	0.9986
<i>S00_072</i>	452.5	7.750	1.439	0.9990
<i>S00_108</i>	451.3	8.050	1.479	0.9989
<i>S00_144</i>	449.8	8.324	1.507	0.9990
<i>S00_180</i>	449.5	8.556	1.524	0.9991
<i>S12_000</i>	377.7	9.706	1.861	0.9989
<i>S12_050</i>	374.3	10.09	1.928	0.9989
<i>S12_100</i>	374.6	10.43	1.937	0.9991
<i>S12_150</i>	370.1	10.83	1.991	0.9991
<i>S12_200</i>	367.3	11.23	2.049	0.9991
<i>S12_250</i>	368.3	11.56	2.094	0.9991
<i>S20_000</i>	333.4	10.74	1.952	0.9993
<i>S20_058</i>	331.0	11.21	2.006	0.9993
<i>S20_116</i>	329.2	11.74	2.074	0.9993
<i>S20_174</i>	330.2	12.02	2.101	0.9993
<i>S20_232</i>	326.0	12.49	2.171	0.9992
<i>S20_290</i>	323.1	13.04	2.262	0.9990
<i>S35_000</i>	272.2	11.58	1.925	0.9996
<i>S35_072</i>	271.0	12.10	1.988	0.9996
<i>S35_144</i>	265.7	12.66	2.043	0.9992
<i>S35_216</i>	260.9	13.20	2.135	0.9995
<i>S35_288</i>	259.2	13.79	2.170	0.9990
<i>S35_360</i>	253.7	14.41	2.269	0.9990

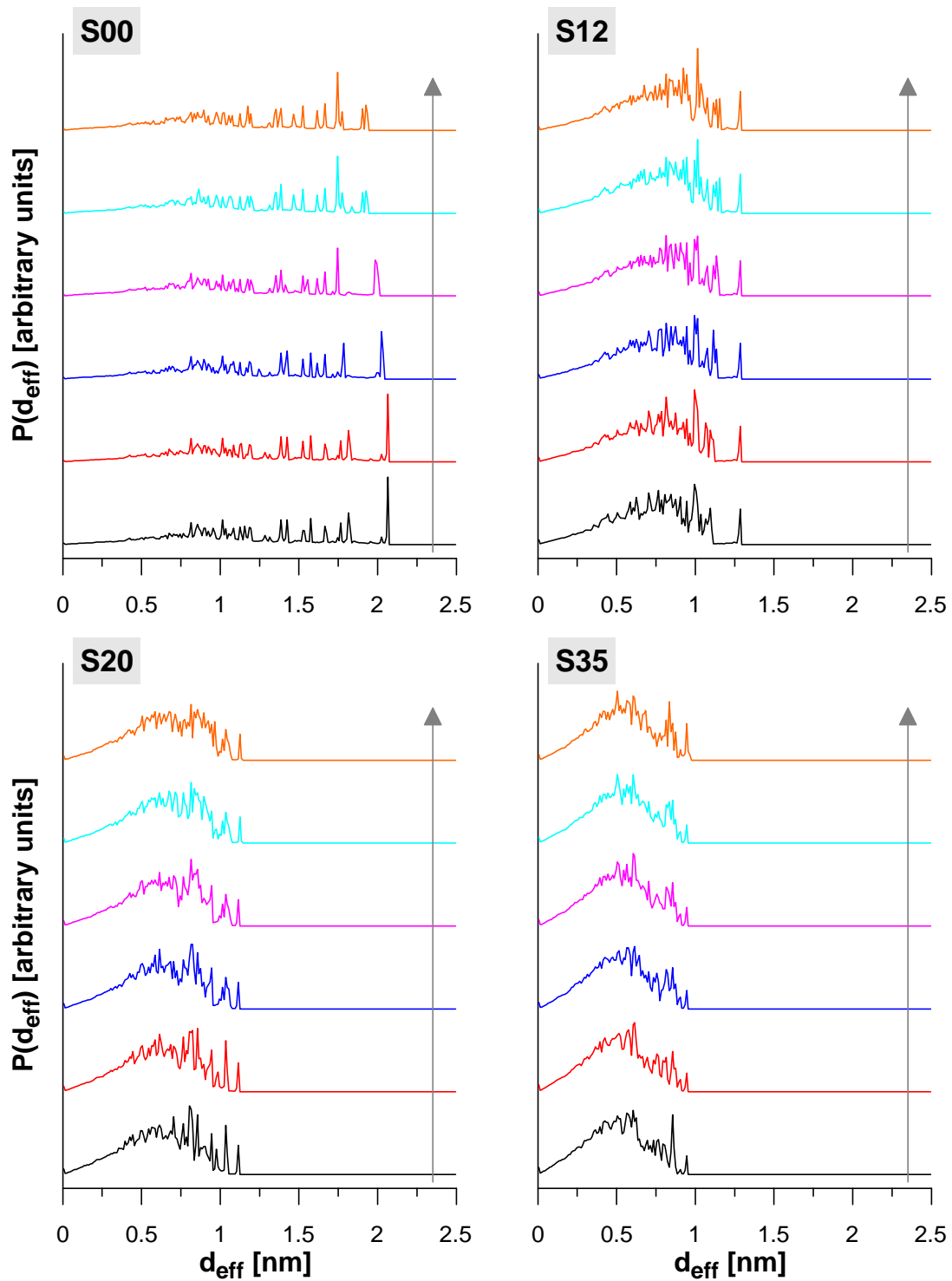


**Fig. 1.** The pore size distribution curves of studied VPC models calculated using Bhattacharya and Gubbins method (for details see [10,11]). Arrows shows the rise in the number of oxygen groups.

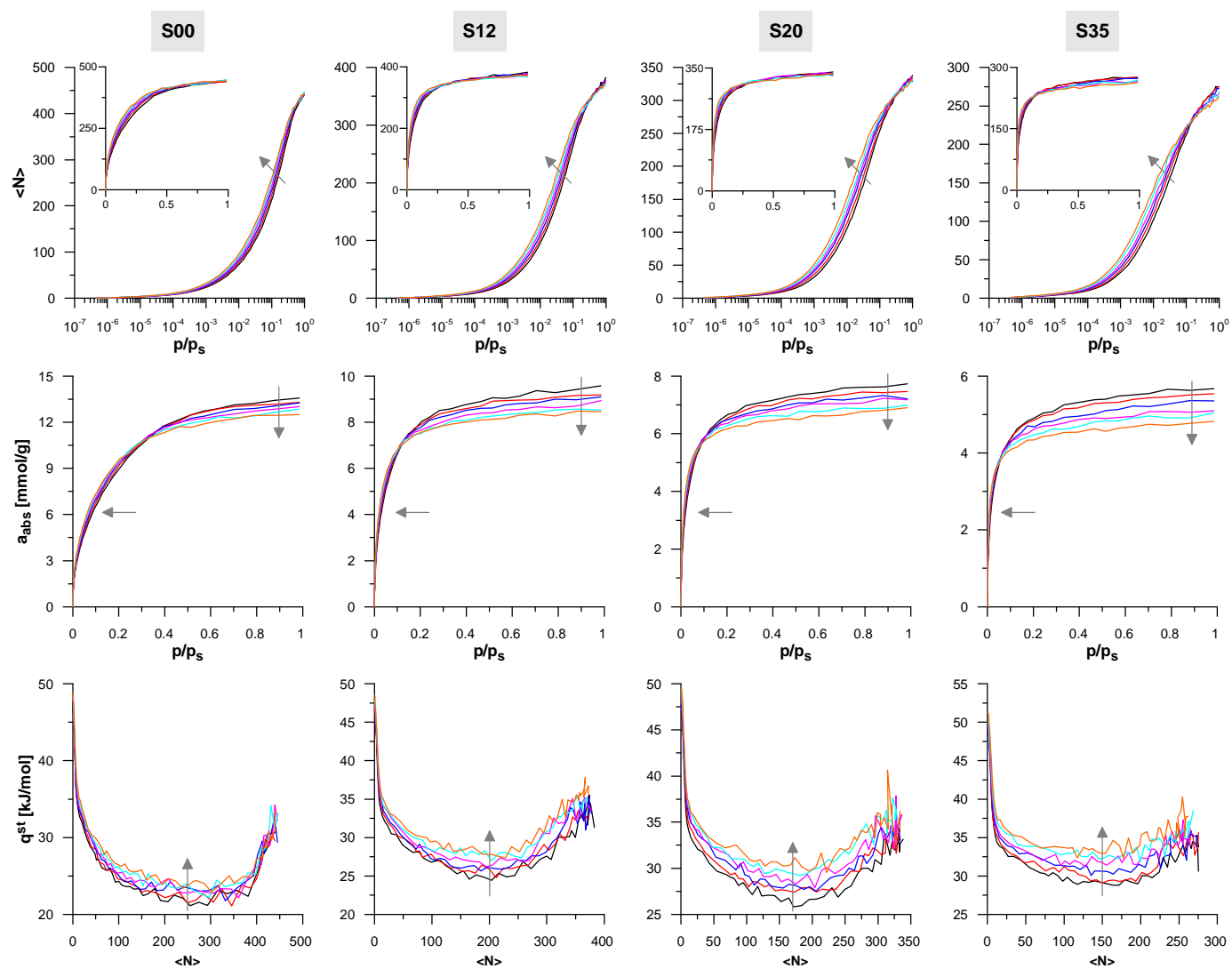


**Fig. 2.** The comparison of adsorption values (the average number of molecules in the box ( $\langle N \rangle$ ) and the absolute adsorption values ( $a_{abs}$ )) and the isosteric enthalpy of adsorption for studied systems. Arrows shows the rise in the number of oxygen groups.

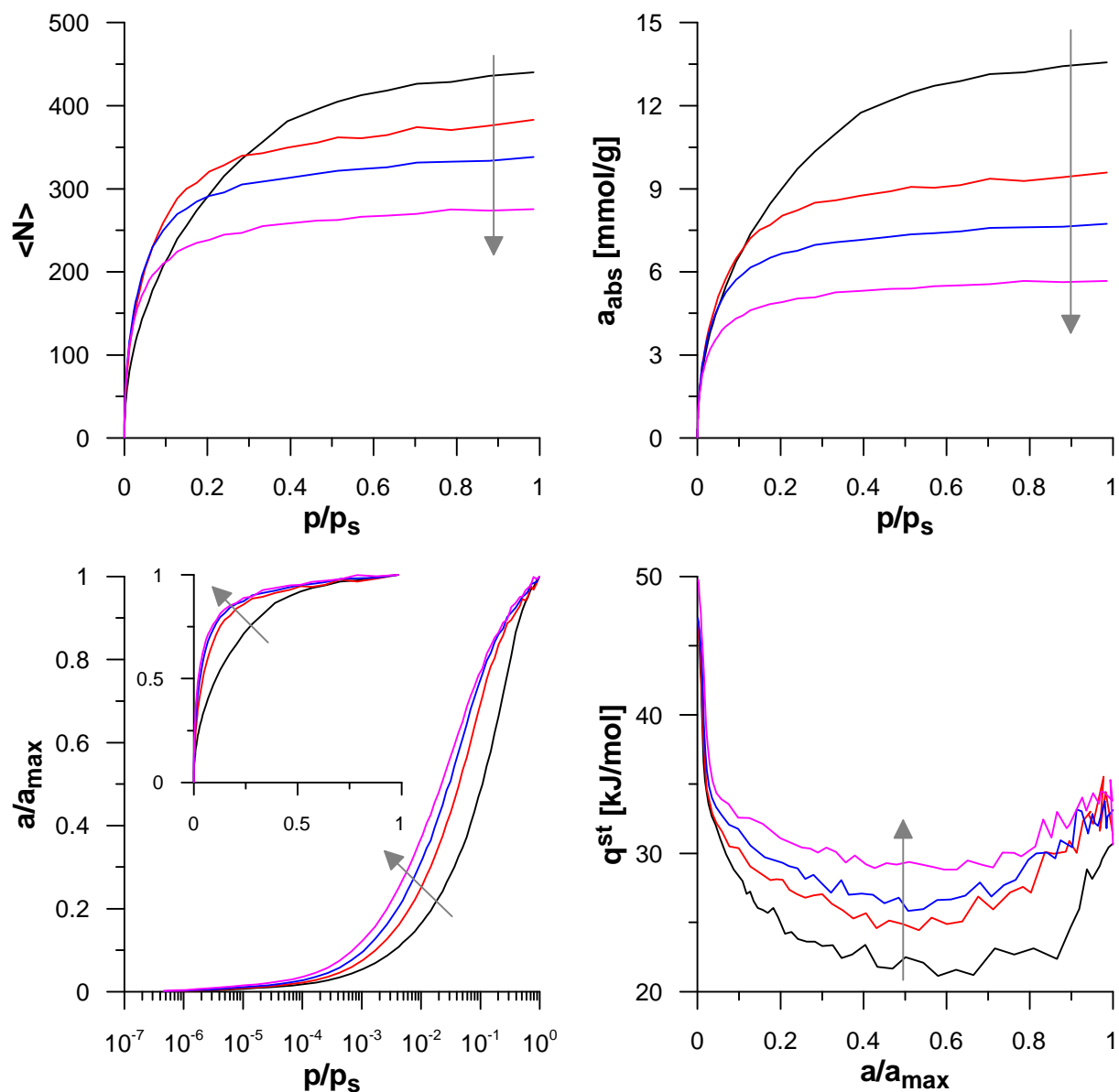


**Fig. 3.** The comparison of adsorption isotherms (the average number of molecules in the box ( $\langle N \rangle$ )), the relative adsorption values and the isosteric enthalpy of adsorption for studied VPC do not containing oxygen (VPCs S00\_000, S12\_000, S20\_000 and S35\_000). Arrows shows the decrease in the average micropore diameter.

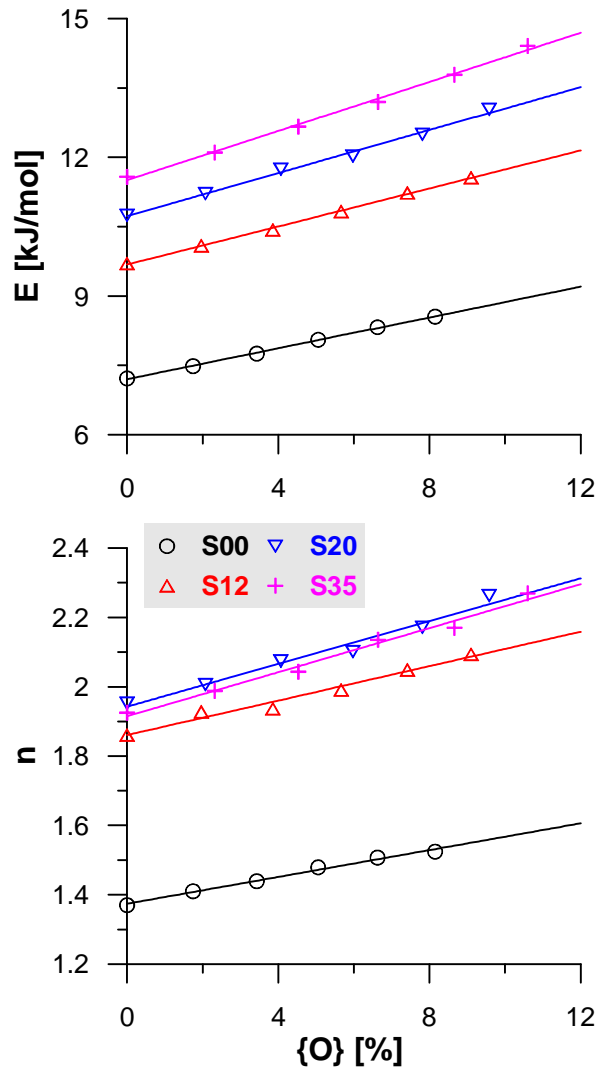


**Fig. 4.** The correlations between the DA equation parameters and the percentage contents of oxygen ({O}) for studied VPC models.

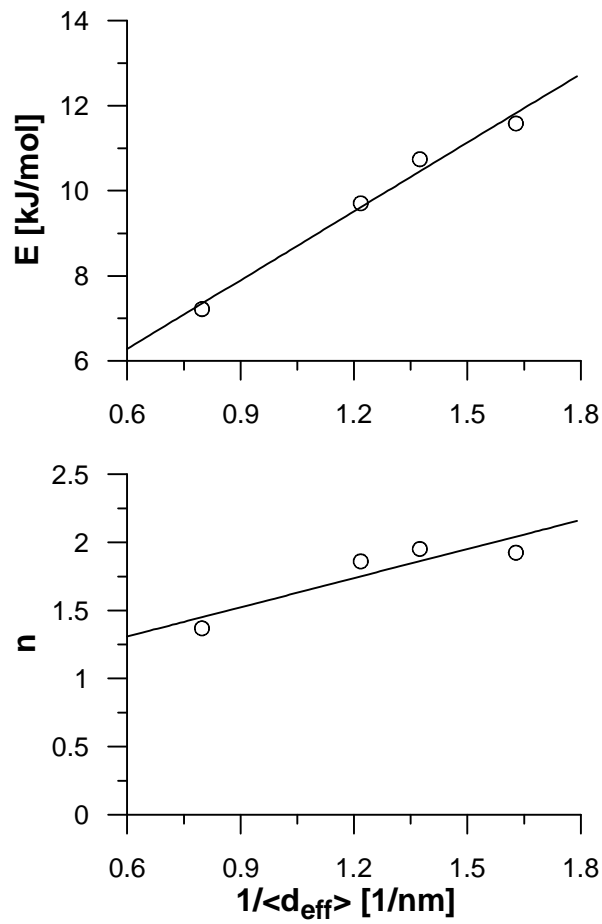


**Fig. 5.** The correlations between the DA equation parameters and the converse micropore diameter ( $1/\langle d_{eff} \rangle$ ) for the VPC models do not containing oxygen.